

# Experimental & Numerical Analysis of Ranque-Hilsch Vortex Tube And Recommendations For Better Operation

Harikrishna Chavhan<sup>1</sup>, Er. Pramod Mandal<sup>2</sup>

<sup>1,2</sup>Dept of Aerospace Engineering

<sup>1,2</sup>Desh Bhagat University

**Abstract-** A vortex tube is a simple device that can separate a single stream of compressed air into two streams, one at a temperature higher than the inlet gas stream and the other at a temperature lower than the inlet stream. Vortex tubes are widely used in cooling applications where compactness, safety, and low equipment cost are basic factors. To better understand gas separation performance, a 3D model of vortex tube was designed using Ansys Workbench, a commercial CFD package. The turbulent flow within the device was modeled using the  $k-\epsilon$  model. Since the aim of this study was to investigate geometric modifications and their impact on the performance of the vortex tube, several changes in the vortex tube geometry was examined. Model validation was achieved using a base vortex tube model and compared to published results. Then the effect of the number of inlet nozzles, Length to tube Diameter ratio ( $L/D$ ), Cold Diameter to tube Diameter ratio ( $(D_c/D)$ ) and Cone valve inner diameter ( $(D_{co}/D)$ ) variation on the performance of the vortex tube were studied. This was followed by examining the introduction of vortex chamber and the effect of the non-dimensional chamber diameter ( $(D_{ch}/D)$ ) on the performance of the vortex tube. Experimental validation tests were also conducted on vortex tube currently on the market and the CFD results were compared.

**Keywords-** CFD Simulation, Parametric Study, Temperature separation, Vortex tube

## I. INTRODUCTION

The vortex tube was invented by a student named G.J Ranque in 1932. He was able to create two streams with different temperatures, using a highly compressed inlet pressure supply. In 1945, a German physicist Rudolf Hilsch improved the vortex tube design of Ranque and he published his work in a scientific paper [2]. This publication of Hilsch was widely read and was very well accepted by the scientific community and thereby the energy separation phenomena in the vortex tube became a topic of great interest. Even though, Hilsch fabricated a less than optimized vortex tube geometry,

he was able to measure the temperature difference between the inlet stream and the outlet streams; however he was not able to explain the physical process behind this effect. This device was later named the Ranque-Hilsch Vortex tube acknowledging the work done by both G.J Ranque and Hilsch.

The vortex tube functions as a device capable of separating a compressed air stream into hot and cold streams with different mass fractions. This phenomenon is referred to as energy (temperature) separation. A vortex tube consists of one or more tangential inlet nozzles, an axial tube with a vortex chamber, a cold gas outlet and a hot gas outlet. Dust free dehumidified compressed air in the range of 5 to 6 bars is injected into the vortex chamber tangentially through the inlet nozzles. As the air accelerates through the inlet nozzles, it exits into a cylindrical section with a high angular velocity which generates an intense swirling flow. The gas then proceeds towards the hot outlet with the conical back pressure control valve (Figure 1). However, not all the flow exits through the control valve. A portion of the gas reverses its direction and moves axially along the center of the tube towards the cold outlet, against the oncoming hot swirling flow.

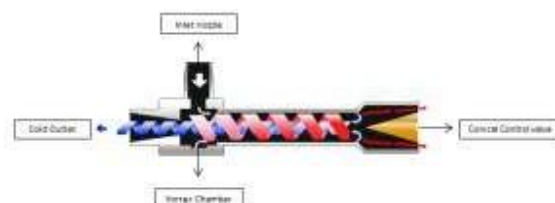


Figure 1: Schematic diagram of a Vortex tube and the phenomena of flow reversal [21]

As the reversed flow move towards the cold exit the thermal energy possessed by the core flow is transferred to the peripheral region of the flow. This results in the peripheral flow temperature exceeding the inlet gas temperature. The peripheral flow exits through the annular space between the tube wall and the conical valve at the hot outlet, whereas the core flow exits through the cold outlet orifice. The relative

mass flow rates of hot and cold gases are controlled by the conical back pressure valve at the hot outlet. This energy separation phenomenon is known as Ranque effect.

Vortex tube is compact, lightweight and is free from any moving part. It does not have any issues related to maintenance as it uses neither electricity nor chemicals. It is cheap compared to other cooling devices and it does not require any refrigerant unlike other localized cooling devices. It is wear resistant as it is made of stainless steel.

It is resistant to corrosion and oxidation as well. The hot side temperature and thereby the total temperature difference can be altered by changing the geometrical settings (conical control valve setting) of the vortex tube. Most importantly it gives instant cold air. But to produce the instant cold air, it requires costly compressed air. Another important factor to note is that the efficiency of this separation mechanism is not very good. But the disadvantages of using the vortex tube are far overpowered by the advantages. Considering these facts it is gradually becoming a very popular device in the industries where localized cooling is required. It is used in electric and electronic industry for cooling CCTV cameras and electronic controls. It is also used for machine part cooling, food item cooling and gas sample cooling. It is used in the industries where quick cooling is of ultimate importance; like setting hot melts and soldered parts. Cooling heat seals and environmental chambers are other applications of vortex tube. It is even used in certain "cryogenic" applications like cooling lab samples and circuit testing.

Although several theories have been formulated to explain the phenomena of temperature separation in the vortex tube, none of them appears to be completely validated. Hilsch [1] proposed that the transfer of tangential shear work from inner to outer fluid layers is the cause of energy separation. Ranque [2] proposed that the work transfer caused by compression and expansion effects is the main reasons for the temperature separation in the tube. Harnett and Eckert [3] suggested that invoked turbulent eddies are responsible for the temperature separation mechanism in the vortex tube. Since turbulent motion has a wide spectrum of eddy sizes, and large eddies (associated with LOW frequency fluctuations) and small eddies (associated with HIGH frequency fluctuations) can coexist in the same volume of fluid, they suggest that the wide spectrum of eddies are the reason for the phenomena of temperature separation. Ahlborn and Groves [4] proposed that the embedded secondary circulation is the phenomena that cause the energy separation. They measured the axial and azimuthal velocity components to reach this conclusion. Stephan et al. [5] proposed that the formation of Görtler

vortices on the inside wall of the vortex tube is the reason that drives the fluid motion in the vortex tube. Görtler vortices are stream-wise secondary flows that appear in a boundary layer flow along a concave wall. If the boundary layer thickness is comparable to the radius of curvature, the centrifugal action creates a pressure variation across the boundary layer. This leads to the centrifugal instability (Görtler instability) of the boundary layer and consequent formation of Görtler vortices. Kurosaka [6] reported that acoustic streaming effect is the reason for temperature separation. Acoustic streaming is a steady flow in a fluid driven by the absorption of high amplitude acoustic oscillations. It is the less-known and opposite of sound generation produced by a flow.

Numerous research activities were conducted on vortex tube over the years. Aljuwayhel et al. [7] investigated the energy separation mechanism using the fluid dynamics model of the vortex tube. Scheper [8] used probes and visualization techniques to carry out an experimental study. They measured the total temperature gradient, velocity and pressure (which were the basic flow parameters measured) and concluded that the axial and radial components of velocity were much smaller than the tangential velocity. Takahama and Yokosawa [9] examined the possibility of shortening the vortex tube chamber length by introducing diverging section for the vortex chamber. Eiamsa-ard and Promvong [10] conducted experimental studies to investigate the phenomena of energy separation. They used the snail entrance method to inject the compressed air into the vortex chamber. They found that this method improved the cold side temperature drop and thereby improved the efficiency of the vortex tube as well. Although no single process has been conclusively validated, the current work looks at the impact on thermal performance of various parameters.

Table 1: Energy separation in a vortex tube: Theories

Name of the Researcher(s)	Energy separation Theories	Importance of the model
Ranque [2]	Work transfer caused by compression and expansion effects	Discovered the basic vortex tube.
Hilsch [1]	Transfer of tangential shear work from inner to outer fluid layers	Presented a modified and improved version of Ranque's vortex tube
Hamett and Eckert [3]	Invoked turbulent eddies	Presented a model based on turbulent rotating flow with solid body rotation
Ahlborn and Groves [4]	Embedded secondary circulation	Introduced an analytical model which was experimentally validated
Stephan et al. [5]	Formation of Görtler vortices on the inside wall of the vortex tube	Introduced the idea of stream-wise secondary flows
Kurosaka [6]	Acoustic streaming effect	Introduced the idea of temperature separation by attenuated sound waves.

Table 2: Major Studies conducted on Vortex Tube

Name of the Researcher(s)	Study Conducted	Importance of the study
Aljuwayhelet al. [7]	Used the fluid dynamics model of the vortex tube	The study showed that the work transfers separates the cold flow region and the hot flow region
Scheper [8]	Used probes and visualization techniques	Experimental study showed that the axial and radial components of velocity were much smaller than the tangential velocity
Takahama and Yokosawa [9]	Shortened the vortex tube chamber length	Introduced a diverging section for the vortex chamber. This improved the thermal performance
Eiamsa-ard and Promvonge [10]	Conducted experimental studies	Used snail entrance method to inject the air into the vortex chamber. This improved the cold side temperature drop and thereby the efficiency of the vortex tube

Even though several studies were conducted, none of them appears to be conclusive. The analysis of the vortex tube using mathematical or analytical method was of great difficulty considering the complexity of processes present within the vortex tube. The flow is highly irreversible, compressible and viscous. So the mathematical modelling produced results that were highly inconclusive. The aim of the current study was to vary parameters that were never varied before and determine the optimum values which can be used to improve the performance of the vortex tube. The work done

in this study can be divided into two parts. The first part is to conduct a parametric study on the base computational model of the vortex tube, and second validate the CFD model using experimental data obtained on a small commercial vortex tube available.

## II. MATHEMATICAL MODEL

Selecting the right geometry is very important when it comes to the CFD analysis of a vortex tube. Based on the literature survey numerous geometries have been examined and unfortunately, majority of the CFD studies were conducted on two dimensional models [17], [18], [19]. It is stated that the two dimensional modeling with axisymmetric approximation can provide a good approximation of the 3D phenomena. However, the flow behavior in the vortex tube is very complex and highly turbulent. Since these complex 3D vortical effects are absent in the 2D model, it was decided to forgo the axisymmetric approximation and develop a 3D model. Various 3D computational models were considered before finalizing the current geometry. The 3D model used by John Wills et al. [12] was used for the initial validation study. Matching of the results enabled, the vortex model by Wills et al. [12] to serve as the base model for all the geometric modifications that were to be implemented. The geometry used by R. S. Maurya et al. [13] had same geometrical parameters, but they used 6 inlets instead of the 2 inlets used by John Wills et al. [12]. These published results [12] [13] gave us the luxury to compare the results obtained after geometric modifications of the base model, with them whenever possible.

Table 3: Geometrical parameters of the vortex tube used for validation study

Parameters	Values
Vortex Tube Length	120 mm
Number of Nozzles	2
Length to Diameter Ratio (L/D)	10
Inlet Area to Area of the vortex tube Ratio (Ai/A)	0.07
Hot Outlet Area to Area of the vortex tube Ratio (Aho/A)	0.3
Cold Outlet Area to Area of the vortex tube Ratio (Ac/A)	0.34

### A. Meshing Strategy

Meshing was done in Ansys Workbench v 14.5.0. Literature survey [12] [13] was conducted to select the best meshing strategy. For such a complex geometry, an unstructured mesh was preferred, using mainly tetrahedral volumes. Inflation layers were applied to the boundary. The volume elements near the tangential inlet portion of the domain are highly skewed, thus reducing the quality of the

mesh. To eliminate the errors due to coarseness of grid, an analysis of different number of cells was performed. Therefore a grid independence study was performed where the criterion was based on the variation of cold exit temperature and hot exit temperature, as the number of cells was changed.

**B. Assumptions**

To aid the solution of this complex vortical flow field, several simplifying assumptions were made. Specifically, the working medium was assumed to be an ideal gas with adiabatic tube walls. So there is no transfer of heat between the system and the surroundings. No slip conditions were used at the solid boundary and the flow is considered to be highly turbulent. The flow is steady and therefore the system properties are assumed not to change with time. However the flow is compressible and therefore the density of the fluid changes significantly. Body forces were considered to be negligible and the flow was considered to be three dimensional and subsonic with uniform fluid properties at the inlet.

**C. Boundary Conditions**

An appropriate boundary condition is a must for obtaining a successful solution. But, the determination of the appropriate boundary condition can be a very time consuming process. A study of previous works [12] [13] showed that good results were obtained when a pressure or mass flow-rate boundary condition is applied at the inlet of the vortex tube. Highly pressurized gas is injected through the inlet nozzles which separate into two different gas streams; one that exits through the hot side and the other that exits through the cold side. So a pressure boundary condition is considered ideal at the inlets and at the exits. Therefore, a pressure boundary condition is applied to the inlet region (inlet nozzle) of the vortex tube with total pressure of 5bar (gauge) and total temperature of 300 K. Even though the inlet pressure was selected based on the previous studies conducted; the current CFD and experimental validation testing conducted also showed that the inlet pressure of 5 bars produced the highest total temperature difference. From the literature survey conducted [12] [13] it was also clear that relative pressure is imposed at the outflow boundaries; in most of the cases. The earlier studies conducted showed that it was ideal to use atmospheric static pressure at the hot exit. Thus a pressure outlet boundary condition was imposed to the cone valve just upstream to the hot exit of vortex tube (hot outlet) with a pressure of 1bar (gauge). Further, a pressure outlet boundary condition to cold orifice of the vortex tube set a pressure of 0bar (gauge). The operating condition was absolute pressure of 1bar and a temperature of 300K. Due to the fast energy

separation process in the vortex tube the wall was assumed to be adiabatic. Based on the previous CFD studies conducted, it was determined that the tangential speed was below Mach number 1, (sonic speed) inside the vortex tube.

**D. Modeling in Fluent**

In the simulation of compressible turbulent flows, the Navier-stokes equations (2) and (3), energy equations (4) are solved by using a CFD package based on rectangular finite volume method (Ansys Fluent). The solver selected for this simulation was a 3D and steady state, density based implicit solver. A second order discretization technique was employed along with a k-ε model to account for the turbulence.

Table 4: Thermo-physical properties of air

Properties (Working Medium - Air)	Values
Density	Ideal Gas Equation
Specific Heat	1006.43 J/Kg-K
Thermal Conductivity	0.0242 w/m-k
Viscosity	1.7894e-5 kg/m-s

The ideal gas equation can be written as:

$$\frac{P}{\rho} = R T \tag{1}$$

The mass balance, momentum balance and energy balance equations are given as:

$$\frac{\partial \rho}{\partial t} + \nabla \cdot \rho u = 0 \tag{2}$$

$$\frac{\partial \rho u}{\partial t} + \nabla \cdot \rho u u = -\nabla p + \mu \nabla^2 u \tag{3}$$

$$\rho C_p \frac{\partial T}{\partial t} + \nabla \cdot u T = k \nabla^2 T \tag{4}$$

To tackle the phenomena of turbulence, the moreadvanced turbulence models such as the Reynolds stress equations as well as the random number generation k-ε turbulence model were investigated. It was found that these models could not be made to converge for this simulation. Bramo et al. [14] showed that, because of good agreement of numerical results with the experimental the k-ε model with standard wall functions can be selected to simulate the effect of turbulence inside the vortex tube, computational domain.

Since the k-ε model was developed in the early 1970s its advantages and disadvantages is well documented. It is the

simplest of the two equation model to implement. The solution converges relatively easy and it provides reasonable predictions for many physical flows. The k-ε model is valid only for turbulent flows and it can be used in highly turbulent applications. For the k-ε turbulence model the equations (5) and (6), for turbulent kinetic energy k and dissipation ε are solved by using Ansys Fluent.

$$\frac{\partial(\rho k)}{\partial t} + \frac{\partial(\rho k u_i)}{\partial x_i} = \frac{\partial}{\partial x_j} \left[ \frac{\mu_t}{\sigma_k} \frac{\partial k}{\partial x_j} \right] + 2\mu_t E_{ij} E_{ij} - \rho \epsilon \tag{5}$$

$$\frac{\partial(\rho \epsilon)}{\partial t} + \frac{\partial(\rho \epsilon u_i)}{\partial x_i} = \frac{\partial}{\partial x_j} \left[ \frac{\mu_t}{\sigma_\epsilon} \frac{\partial \epsilon}{\partial x_j} \right] + C_{1\epsilon} \frac{\epsilon}{k} 2\mu_t E_{ij} E_{ij} - C_{2\epsilon} \epsilon \frac{\epsilon^2}{k} \tag{6}$$

**III. EXPERIMENTAL VALIDATION STUDY**

The experiment was conducted using the Small Vortex Tube Kit from Streamtek Corp. (Figure 2a). The vortex tube had three generators with different cold diameters, provided with it. The generator is an interchangeable, stationary part in the commercial vortex tube that regulates the volume of compressed air and also the temperature ranges that one can produce using the tube (Figure 2b). The generators are one of the most important components in the vortex tube as they decide the diameter of the cold side and also the number of nozzles. The nozzles are modeled as slits in a generator. Air is supplied to the inlet of the vortex tube from a pressurized chamber. A pressure transducer is used to read the inlet static pressure. Mass flowmeters provided at the inlet and the hot outlet is used to measure the inlet mass flow rate and the hot outlet flow rate. Thermocouples connected to a multimeter provided the temperature measurements at the cold and hot exits of the vortex tube.

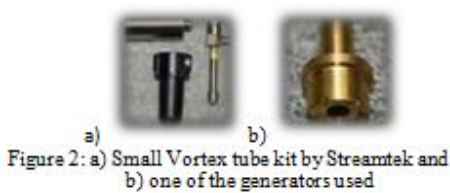


Figure 3: Test stand setup for the experimental validation study

The vortex tube had three generators provided with it and based on the experimental study conducted it was concluded that the generator with a cold diameter of 4 mm provided highest temperature difference. The generator had 6 slits (rectangular inlets). The inlet air with pressures ranging from 1.37 bar (20 psi) to 4.83 bar (70 psi) was injected into the vortex tube inlet. The inlet and the hot outlet mass flow rates were separately measured using temperature corrected flowmeters provided at the inlet and hot outlet. The corresponding cold outlet and hot outlet temperatures were acquired by using the thermocouples-multimeter combination. An average of ten readings was taken for each of the inlet pressure input, at the hot side and the cold side. The hot side total temperature, cold side total temperature and the corresponding total temperature difference for different inlet pressures were noted.

The Cold end total Temperature Difference is the temperature difference ( $\Delta T_c$ ) between the inlet gas total temperature ( $T_i$ ) and the cold side gas total temperature ( $T_c$ ), and the Hot end total Temperature Difference ( $\Delta T_h$ ) is the temperature difference between the inlet gas total temperature ( $T_i$ ) and the hot side gas total temperature ( $T_h$ ).

$$\Delta T_c = T_i - T_c \tag{7}$$

$$\Delta T_h = T_i - T_h \tag{8}$$

The Total Temperature Difference ( $\Delta T$ ) is the temperature difference between the cold side gas total temperature ( $T_c$ ) and the hot side gas total temperature ( $T_h$ ).

**IV. RESULTS AND DISCUSSIONS**

**A. Grid Independence Study**

The mesh (cell) size was varied from 16,445 to 212,464, based on changes in the total temperature difference. While the cold side temperature approached an asymptotic state for a mesh size of 123,598, the hot side temperature approached the asymptotic state when the cell number was increased to 176,728. Therefore it can be clearly seen from the total temperature difference (Figure 4) plot that there is an advantage in increasing the number of cells to 176,728 for the configurations studied.

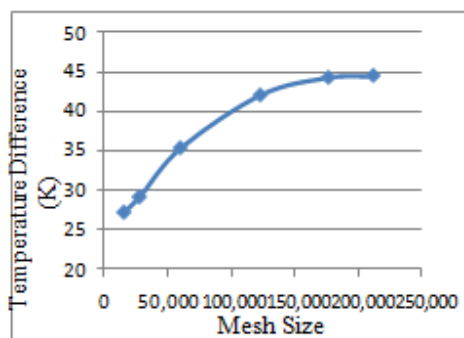


Figure 4: The total temperature difference variation with the number of cells

**B. Validation Study**

**(a) Flow physics study**

To understand the flow physics inside the vortex tube, the tangential (swirl) velocity was plotted along the radius of the tube. The plot obtained clearly shows that the vortex system generated in the vortex tube is a combination of both a forced vortex and free vortex. The forced vortex is formed around the vortex tube center and free vortex is formed near the vortex tube walls.

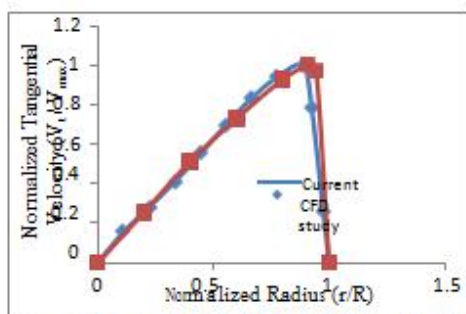


Figure 5: The tangential (swirl) velocity along the radius (normalized) at X/L=0.5

The above plot provides an indication of the tangential velocity variation along the radius for the base model, at X/L = 0.5. The current study is compared with the work of Dutta et al. [25]. The tangential velocity is normalized by dividing the local tangential velocity at each radial location by the maximum tangential velocity, in both the cases. Both studies show the same trend and are within 5% of one another, at X/L = 0.5. For the current study, the maximum tangential velocity approaches a Mach number of 0.5 approximately at the given location (X/L=0.5).

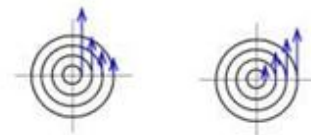


Figure 6: Two examples of vortices: a) Free vortex and b) Forced vortex [23]

In figure 6 the velocity distributions that forms in the vortex tube is presented. These two types of vortices are referred to as; free vortex and forced vortex. In the free vortex the peripheral velocity is inversely proportional to the radius (Figure 6a) and in forced vortex the peripheral velocity is proportional to the radius (Figure 6b). Thus the swirling flow in the vortex tube can be characterized as a Rankine vortex because of the presence of a forced vortex in the central core, and a free vortex surrounding it.

The next step in the vortex tube flow physics study is the proof of conservation of energy. The law of conservation of energy states that the total energy of an isolated system remains a constant. The energy equation is given by:

$$E = mC_p \Delta T \tag{9}$$

Therefore, for energy conservation in the vortex tube,

$$m_c C_p T_1 = m_c C_p T_c + m_h C_p T_h \tag{10}$$

The energy calculation is given in table 5 and it shows that the energy contained within the hot and cold flows is within 5% of the supply energy, for the base model, and thereby satisfying the conservation of energy.

Table 5: The total temperature difference variation with the number of cells

Flow Properties	Mass flow rate (kg/S)	Temperature (K)	Energy (J)
Inlet	0.01897	300	5736.65
Cold Outlet	0.01024	270.516	2777.01
Hot outlet	0.00873	313.669	2728.92

(b) Base Model Validation Study

To prove confidence in the current base model used in the present study, the computed CFD results were compared with the results obtained by John Willset al. [12]. Matching of the results enabled, the current vortex tube model to serve as the baseline model for all the geometric modifications that were to be implemented. A 3D replica of the model was designed according to the specifications given by Willset al. [12]. However, the meshing tool and the meshing method were different from the ones provided in his paper. Comparison of the current total temperature contours to those found in Wills et al. are presented and found to be in very good agreement.

Specifically, the peripheral total hot temperature and the core total cold temperature were computed along the axial length and compared. In the current computation, the temperature contour (Figure 8) indicates that the maximum hot side total temperature is 314 K and the minimum cold side total temperature is 270 K. When the contours obtained for the present study was compared with Wills et al. [12] contours in Figure 8; (hot side temperature of 312 K and the cold side temperature of 271 K), the deviation was found to be less than 5 %.

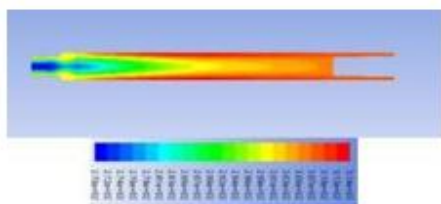


Figure 7: Total Temperature - current CFD study

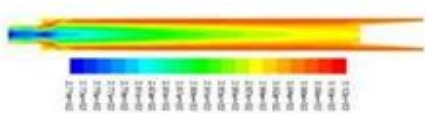


Figure 8: Total Temperature - John Wills et al. [12] study

(c) Experimental Validation Study

In this section, the current computational model was modified to match the geometrical conditions of a

commercially purchased vortex tube which underwent testing and is used for model validation. The geometrical parameters of the commercially purchased vortex tube are given in Table 4. Meshing was again performed using Ansys workbench meshing tool and solving was performed using Ansys Fluent. The meshing and the solving technique used here was exactly same to the one that was used for the base model, in the initial phase of this study. A 3D and steady state, density based implicit solver was used. Second order special discretization technique was used in this analysis along with standard k-ε model with standard wall functions.

The hot side and the cold side temperatures were experimentally acquired and used as the validation data for the CFD simulation. It can be noted that the temperature difference increases linearly with the increase in pressure for the experimental validation study. The CFD results obtained also follows an increasing trend. But the temperature difference plot for the CFD study is not linear as in the case of the experimental validation study. The lowest temperature difference obtained in the CFD study was 26.15 K while the highest temperature difference was 55.52 K.

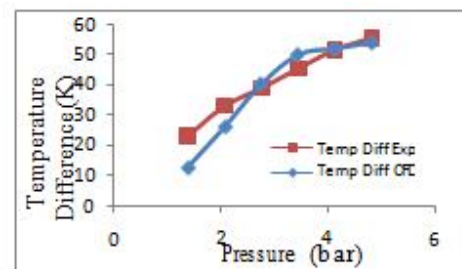


Figure 9: Total temperature difference variation with Pressure

Table 6: Geometrical parameters of the small Vortex Tube from Streamtek Corp. used for experimental validation study

Parameters	Values
Vortex Tube Diameter	6 mm
Number of Nozzles	6
Length to Diameter Ratio (L/D)	18
Inlet Area to Area of the vortex tube Ratio (Ai/A)	0.0277
Hot Outlet Area to Area of the vortex tube Ratio (Aho/A)	0.1736
Cold Outlet Area to Area of the vortex tube Ratio (Ac/A)	0.444

C. Parametric Study

In this section, a computational model was generated with the exact dimensions provided by Willset al. [12] and a parametric study was performed. The impact of varying the geometrical parameters like vortex tube length to diameter ratio (L/D), number of inlets, Chamber Diameter to Diameter

ratio ( $D_{ch}/D$ ), cone valve inner diameter to vortex tube diameter ratio ( $D_{co}/D$ ) and Cold diameter to Diameter ratio ( $D_c/D$ ) on the thermal performance of the vortex tube were evaluated. In the current study the inlet pressure was varied from 2 bars to 6 bars gauge. The results showed that the hot side temperature increases and cold side temperature decreases as the inlet pressure was increased. However, the hot and cold side temperature curves reach an asymptotic state as an inlet pressure of 5 bars gauge is attained; thus clearly demonstrating inlet pressure above 5 bar gauge is not efficient. As a result, the inlet pressure of 5 bar was maintained for all the remaining computations.

(a) Length to Diameter Study

The length of the vortex tube was varied from 40mm to 240mm, while keeping all other geometrical parameters constant. This equated to a non-dimensional length variation ( $L/D$ ) from 3.33 to 20. The total temperature difference rises with increasing tube length and finally it reaches an asymptotic state. The asymptotic state is achieved when  $L/D$  ratio becomes 10. Increasing the  $L/D$  ratio from 10 to 20 gives a total temperature difference rise of just 0.8283 K. Since industries prefer the vortex tube to be compact and light weight, the length of the vortex tube should be kept as small as possible. Therefore, increasing the  $L/D$  ratio more than 10 to produce this slight improvement is not recommended.

Now, to enable a comparison to published work [13], the effect of variation of  $L/D$  on different number of inlets was also studied. The number of inlet nozzles was increased from 2 (base model) to 6. Computations were then conducted to determine the total temperature difference for different  $L/D$  configurations; for the 6 inlet model. The number of nozzles in the base model was then increased to 4 and simulations were run to obtain the Temperature difference for Length to Diameter ratio of 10. Results for the 2, 4 and the 6 inlet case were then compared with the CFD results in the published work [13].



Figure 10: Vortex Tube: Length to Diameter ratio study

It can be noted from the study conducted that, the 2 inlet case reaches an asymptotic state after an  $L/D$  ratio of 10 is achieved. The same trend can be observed in the current 6 inlets study as well. It can also be noted that the temperature difference obtained in the current 2 inlet study is lower than that of the current 6 inlet study, when  $L/D$  is less than 10. But

when  $L/D$  is greater than 10 the temperature difference is almost the same for both 2 inlet and 6 inlet arrangement. The total temperature difference for different  $L/D$  ratios showed that the current 6 inlet study compares very well with the 6 inlet study of Maurya et al. [13] with differences within 10 %. It can also be observed that, for an  $L/D$  ratio of 10 the temperature difference obtained for the 4 inlet case shows no difference with the 2 and 6 inlet study.

Beyond an  $L/D$  ratio of 10, no significant improvement in the temperature difference is observed. Maurya et al. [13] showed that the  $L/D$  ratio should be  $\geq 10$  for maximum energy separation. Their results suggested that the formation of stagnation zone is responsible for this phenomenon. For the vortex tube configuration studied, the stagnation zone formation occurs after the  $L/D$  ratio of 10 is achieved, which is in accordance with Maurya et al. result. In the current  $L/D$  variation study, it can be noted that even for the 6 inlet configuration, the stagnation zone formation occurred after an  $L/D$  ratio of 10 was achieved.

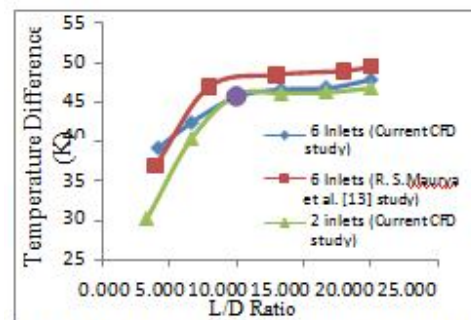


Figure 11: Total temperature difference curve for different  $L/D$  ratios

(b) Number of Inlets :

The base model used for the current study had 2 inlets. To study the effect of change due to the number of inlet nozzles, we considered four nozzle arrangements: 1inlet, 2inlets, 4 inlets and 6 inlets. All the other geometrical parameters were kept constant. The hot side temperature increased considerably, as the number of inlets was increase from one to two. The cold side temperature dropped as the number of inlets was increased from 1 to 2. As the number of inlets is increased from 2 to 4, the total temperature remained almost the same for both hot and cold side.



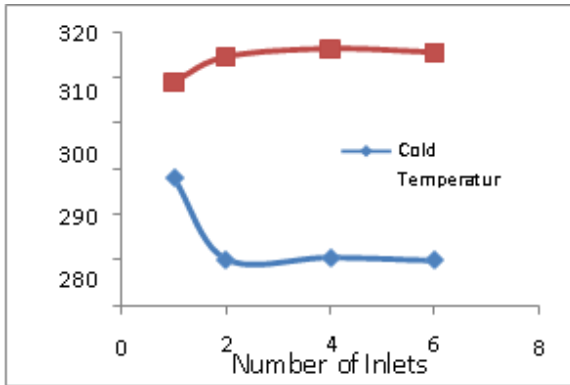


Figure 12: Total temperature variation with number of Inlets

This behavior can be attributed to the Coefficient of Performance (COP). The COP of a vortex tube can be defined in terms of heating (COP<sub>H</sub>) or cooling (COP<sub>R</sub>) and it relates the compression energy required to produce the desired temperature change. COP<sub>H</sub> is defined as the Coefficient of Performance of heating and COP<sub>R</sub> is defined as the Coefficient of Performance of refrigeration. The value of COP increases as the number of inlets was increased from 1 to 2. But this trend is not consistent with the increase in number of inlets. It reaches a maximum somewhere in between.

$$COP = \frac{\text{Desired Output}}{\text{Required Output}} \quad (11)$$

$$COP_R = \frac{\dot{m}_c C_p (T_1 - T_c)}{\dot{m}_1 R T_1 \ln(P_1/P_{atm})} \quad (12)$$

Equation 12 is rearranged into equation 13 to produce a few non-dimensional terms:

$$COP_R = \eta_c \left( \frac{C_p}{R} \right) \left( \frac{1 - T_c/T_1}{\ln(P_1/P_{atm})} \right) \quad (13)$$

The inlet mass flow rate held constant for all the cases considered. Because of this, for a low number of inlets, the resulting pressure loss is high. Thus the energy remaining for vortex generation is not sufficiently strong to support the energy separation. However, at high number of nozzles, since more nozzles are available to inject the compressed air, the air velocity exiting the nozzle is reduced and also has a negative effect on the temperature separation phenomena [16].

Thus for 2, 4, and 6 inlet case, a balance between the pressure drop across the inlet nozzles and nozzle outlet velocity must be obtained, so that the total temperature remains almost constant for these three cases. Whereas for the 1 inlet case the pressure loss is very high compared to the other three cases and therefore the advantage of higher nozzle

outlet velocity is not able to improve the performance of the vortex tube.

The total temperature difference increased considerably as the number of inlets was increased from one to two. But the increase in the temperature difference was only 1.4 K as the number of nozzles was increased from two to four. An increase to 6 nozzles did not show any noticeable change in the temperature difference.

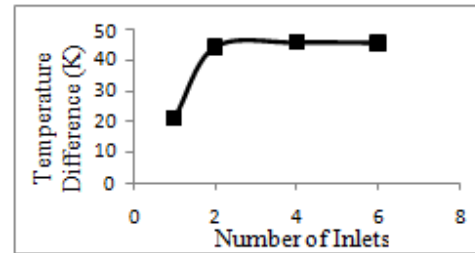


Figure 13: Total temperature difference variation with number of Inlets

It is therefore concluded that using 4 or 6 nozzles in the current vortex tube geometry appears to provide the same temperature difference. In a similar arrangement the vortex tube used for the experimental validation study also, had six inlets and therefore the remaining computational simulations utilized the 6 inlet arrangement. So this study justifies the use of six inlets for the computational simulation of the vortex tube model used for the experiment.

(c) Chamber Diameter to Diameter ratio:

The base model did not have a separate vortex chamber. It was a long tube with a cold outlet section of different diameter and a hot outlet with a conical control valve. However, in this portion of the study, a vortex chamber was introduced. In the literature review conducted [22], it was learned that the vortex chamber (swirl chamber) is the region where the air injected through the inlet, accelerates to achieve a high rate of rotation. Even though the concept of a vortex chamber was already known, no previous studies were conducted on the impact of chamber diameter variations. Thus, the new geometrical parameter to be considered here is D<sub>ch</sub>/D. To study the impact of the introduction of the vortex chamber into the base model, five cases were considered. The first case is the default case with no chamber (D<sub>ch</sub>/D = 1) and the fifth case had a D<sub>ch</sub>/D ratio of 1.66. The other three cases considered were D<sub>ch</sub>/D ratio of 1.167, 1.33 and 1.5.



Figure 14: Vortex tube diagram with the vortex chamber added to the base geometry

The hot side temperature increased till  $D_{ch}/D$  was 1.5 and it started dropping after that (Figure 15). It can also be noted that the cold side temperature increased with the increase in the chamber diameter.

The introduction of a vortex chamber increases the spin generated in the vortex tube. Higher spin causes the fluid particles in the peripheral layer to move faster. This results in an increased hot outlet temperature. Simultaneously the air in the inner core transfers the kinetic energy it possesses to the hot stream and moves out through the cold orifice. Due to this, the air in the inner core region cools down and thereby the air in the peripheral region heats up further. Thus, as the diameter of the vortex chamber increase, the hot side temperature increases till a point where the vortex chamber diameter geometry affected the vortex formation (Figure 15). But the temperature drop in the cold side is not as significant as the hot side. After a  $D_{ch}/D$  value of 1.5, the vortex efficiency is observed to drop and therefore the hot side temperature also goes down.

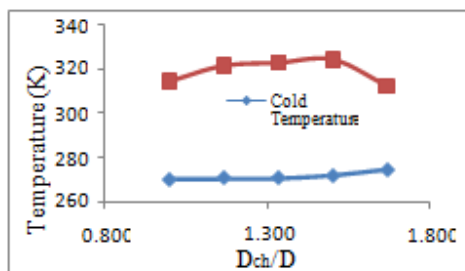


Figure 15: Total temperature variation with Chamber Diameter

Now, if we take a look at the total temperature difference; it started rising till the  $D_{ch}/D$  value was 1.5 and then it dropped to a really low value of 37.76 K. The increase in the temperature difference can be attributed to increase in the tangential velocity due to the chamber diameter increase. The total temperature drop after a  $D_{ch}/D$  ratio of 1.5 can be attributed to decrease in spin efficiency due to increase in vortex diameter beyond an optimum value.

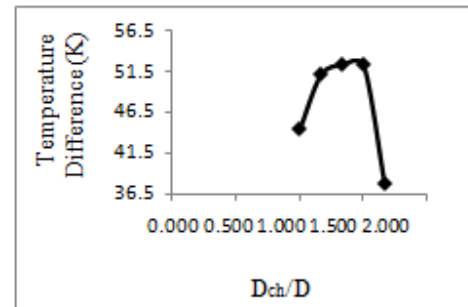


Figure 16: Total temperature difference variation with Chamber Diameter

The vortex chamber cross section for two cases ( $D_{ch}/D= 1.166$  and  $D_{ch}/D= 2.33$ ) were considered. The vorticity contour for  $D_{ch}/D$  of 1.166 is shown in Figure 17. The decrease in total temperature difference after  $D_{ch}/D$  of 1.5 show that there is a decrease in swirl efficiency after the chamber diameter of 18 mm ( $D_{ch}/D$  of 1.5) is achieved. The decrease in swirling motion efficiency can be clearly observed in the vorticity contour for  $D_{ch}/D=2.33$  (Figure 18). This validates the two statements made earlier. The first is that the increase in the vortex chamber (swirl chamber) diameter increases the swirl generated in the vortex tube till a certain point where the vortex geometry affects the temperature separation phenomena and the second one is that the swirl efficiency goes down as the chamber diameter was increased beyond 18 ( $D_{ch}/D= 1.5$ ).

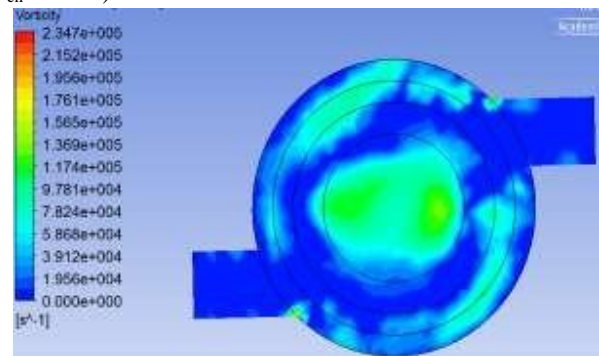


Figure 17: Vorticity contour at Chamber dia = 14mm ( $D_{ch}/D= 1.166$ )

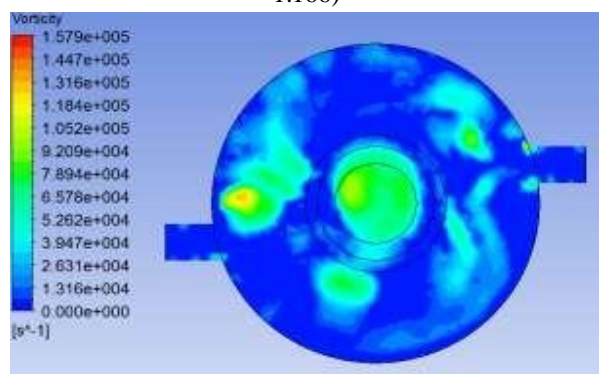


Figure 18: Vorticity contour at Chamber dia = 28mm ( $D_{ch}/D= 2.333$ )

(d) Cone Valve Inner Diameter to Diameter ratio:

In this section of the study, the inner diameter of the cone valve was altered. Six cases were considered including the default case to investigate the effect of change of the inner cone diameter. All other geometrical parameters, including the outer diameter of the cone valve, were kept the same as in the base model. Thus, the geometrical parameter to be considered here is the  $D_{co}/D$  (Figure 19). The smallest  $D_{co}/D$  considered was 0.167 and in that case the cone valve geometry was close to a cone. The biggest  $D_{co}/D$  considered was 0.833 and in that case the cone valve geometry was close to a cylinder. This will be the first published study, to present this effect.

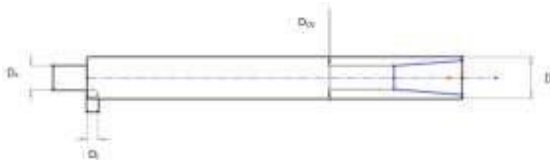


Figure 19: Vortex tube diagram with the representation of cone valve inner diameter

The cold side temperature increases as the cone diameter increases. It reaches the highest value of 274.1 K for a  $D_{co}/D$  value of 0.5 and then it gradually decreases. When the cone diameter gradually approaches the value of the vortex tube diameter, the rise in the cold side temperature (although very small) can be observed. The hot side temperature decreases as the cone diameter increases. It reaches the lowest value of 314.12 K for a  $D_{co}/D$  value of 0.5 and then it gradually increases. When the cone diameter gradually approaches the value of the vortex tube diameter, the hot side temperature reaches an asymptotic state.

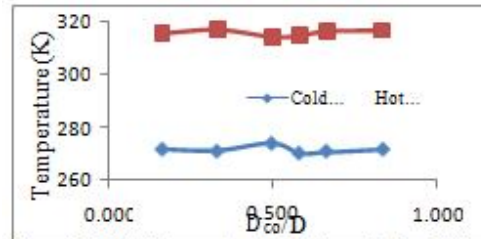


Figure 20: Total temperature variation with Cone Valve Inner Diameter

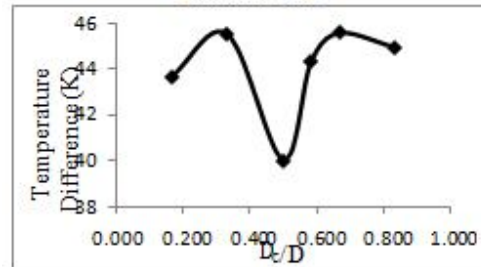


Figure 21: Total temperature difference variation with Cone Valve Inner Diameter

The total temperature difference shows that at very small  $D_{co}/D$  and at very high  $D_{co}/D$  (when cone diameter almost approach the vortex tube diameter) the temperature difference is low. But the lowest value of temperature difference is found at a  $D_{co}/D$  value of 0.5. Thus the ideal  $D_{co}/D$  was found to be 0.667.

(e) Cold Diameter Change

Cold end orifice diameter is another important geometrical parameter that affects the thermal performance of the vortex tube. Six orifice diameter cases were considered including the default case of  $D_c/D$  of 0.583.

As the cold diameter increases, the hot side temperature initially drops and then rises. This increasing trend is stopped at  $D_c/D$  of 0.667, where another drop begins to occur. Cold exit temperature initially drops till  $D_c/D$  is 0.667 and then there is a steep increase in the cold side temperature as the cold orifice diameter increases. The lowest cold side temperature was obtained at the default 7mm orifice diameter case ( $D_c/D = 0.583$ ). The total temperature difference therefore attains its highest value at  $D_c/D$  of 0.667 and after that it drops. It reaches the lowest value at cold diameter of 10mm ( $D_c/D = 0.833$ ) which is very close to the vortex tube diameter.

Maurya et al. [13] suggests that the reduction in pressure gradient causes energy separation as well as supply air with cold air mixing, at the cold orifice. This reduction in pressure gradient is the reason for rising cold temperature according to them. The rise in cold temperature beyond  $D_c/D$  ratio of 0.583 in the current study can therefore be attributed

to reduction in the pressure gradient. They also suggest that the radial pressure gradient increase which leads to more energy separation is the reason for the falling cold temperature. In the current study a clear drop in the cold temperature can be seen from  $D_c/D$  ratio of 0.5 to 0.583. Therefore, the current study agrees very well with the Maurya et al. study.

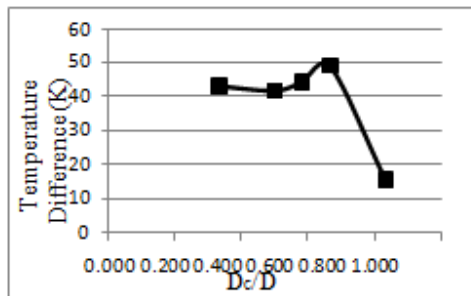


Figure 22: Total temperature difference variation with Cold Diameter

## V. SUMMARY

A reference validation study was conducted to provide confidence in the current model. This was achieved, by comparing the contours obtained in the current study with those of Wills et al. [12]. Since the deviation in results were within 5%, the vortex model of Wills et al. was used as the base model for all the geometric modifications that were to be examined in the present study. A geometric parametric study on the base computational model of the vortex tube was done. From the current parametric study, it was concluded that the:

- i. Ideal chamber diameter to Diameter ratio ( $D_{ch}/D$ ) for the vortex tube studied was 1.5.
- ii. The ideal cone diameter to Diameter ratio ( $D$  for the vortex tube studied was 0.667.co/D)
- iii. The ideal Length to Diameter ratio ( $L/D$ ) for the vortex tube studied was greater than 10.
- iv. Ideal inlet nozzle number for the vortex tube studied was four.
- v. The ideal cold diameter to Diameter ratio ( $D_c/D$ ) for the vortex tube studied was 0.7.

An experimental validation study was conducted on the small Vortex Tube Kit from Streamtek Corp. by comparing the experimental results with the already obtained CFD results. The deviation in cold and hot side temperatures of the experimental study from the CFD results was less than 10%, giving additional confidence to the current CFD model.

## REFERENCE

- [1] G. J. Ranque, "Method and apparatus for obtaining from a fluid under pressure two outputs of fluid at different temperatures," US patent No.1:952, pp.281, 1934.
- [2] R. Hilsch, "The use of expansion of gases in a centrifugal field as a cooling process," Rev. Sci. Instrumentation, vol. 18(2), pp. 108–113, 1947.
- [3] Harnett, J. and E. Eckert, "Experimental study of the velocity and temperature distribution in a high velocity vortex-type flows," Trans. ASME, 79: 751-758.( 1957)
- [4] Ahlborn, B. and J. Gordon, "The vortex tube as a classical thermodynamic refrigeration cycle," J. Appl. Phys., 88: 3645-653.( 2000)
- [5] Stephan, K., S. Lin, M. Durst, F. Huang, D. Seher, "An investigation of energy separation in a vortex tube," Int. J. Heat Mass Transfer, 26: 341-348.( 1983)
- [6] Kurosaka M., "Acoustic streaming in swirling flows". J. Fluid Mech., 124: 139-172.( 1982)
- [7] Aljuwayhel, N.F., G.F. Nellis and S.A. Klein, "Parametric and internal study of the vortex tube using a CFD model," Int. J. Refrig., 28: 442-450.( 2005)
- [8] G.W. Scheper, "The vortex tube; internal flow data and a heat transfer theory," J ASRE Refrig. Eng., vol. 59, pp. 985–989, 1951.
- [9] H. Takahama and H. Yokosawa, "Energy separation in vortex tubes with a divergent chamber," Trans ASME J Heat Transfer, vol. 103, pp. 196–203, 1981.
- [10] S. Eiamsa-ard, and P. Promvonge, "Numerical investigation of the thermal separation in a Ranque–Hilsch vortex tube," Int. J. Heat Mass Transfer, vol. 50(5–6), pp. 821–832, 2007.
- [11] C.U. Linderstrom-Lang, "The three-dimensional distributions of tangential velocity and total-temperature in vortex tubes," J. Fluid Mech., vol. 45, pp.161–187, 1971.
- [12] John Wills. N, Karthika. A. S, "Numerical Analysis of Flow Behavior and Energy Separation in Vortex Tube," 10th National Conference on Technological Trends (NCTT09) 6-7 Nov 2009
- [13] R. S. Maurya, Kunal Y. Bhavsar, "Energy and Flow Separation in the Vortex Tube: A Numerical Investigation," International Journal on Theoretical and Applied Research in Mechanical Engineering
- [14] Bramo, A.R., Pourmahmoud, N, "Computational Fluid Dynamics Simulation of Length to Diameter Ratio Effect on the Energy Separation in a Vortex Tube," Thermal Science, 15(2011), 3, pp. 833-848
- [15] Mohammad O. Hamdan, Basel Alsayed, Emad Elnajjar "Nozzle parameters affecting vortex tube energy separation performance," Heat Mass Transfer, DOI 10.1007/s00231-012-1099-2

- [16] Nader Pourmahmoud&Abdol Reza Bramo “The effect of l/d ratio on the temperature separation in the counter flow vortex tube”
- [17] JiříLinhart, Mohamad Kalal, Richard Matas “Numerical Study Of Vortex Tube Properties”
- [18] C. H. Marquesa, L. A. Isoldia,E. D. dos Santosa,and L. A. O. Rochab, “Constructal design of a vortex tube for several inlet stagnation pressures”
- [19] N.Pourmahmoud, S.Akhesmeh, “Numerical Investigation of the Thermal Separation in a Vortex Tube”
- [20] [http://download.autodesk.com/us/algos/userguide/mergedProjects/setting\\_up\\_the\\_analysis/Fluid\\_Flow/analysis\\_Parameters/Steady\\_or\\_Unsteady\\_Fluid\\_Flow\\_%28Turbulence\\_Options%29.htm](http://download.autodesk.com/us/algos/userguide/mergedProjects/setting_up_the_analysis/Fluid_Flow/analysis_Parameters/Steady_or_Unsteady_Fluid_Flow_%28Turbulence_Options%29.htm)
- [21] <http://www.exair.com/enUS/Primary%20Navigation/Products/Vortex%20Tubes%20and%20Spot%20Cooling>
- [22] [http://en.wikipedia.org/wiki/Vortex\\_tube](http://en.wikipedia.org/wiki/Vortex_tube)
- [23] [http://www.jsme-fed.org/experiment-e/2011\\_2/03.html](http://www.jsme-fed.org/experiment-e/2011_2/03.html)
- [24] Dr.Ing.Ramzi, Raphael IbraheemBarwari,“Effect of Changing Cone Valve Diameter on the performance of Uni-Flow Vortex Tube”
- [25] T. Dutta,K.P. Sinhamahapatra, S.S. Bandyopdhyay"Comparison of different turbulence models in predicting the temperature separation in a Ranque–Hilsch vortex tube"